Interaction of Tubulin with a New Fluorescent Analogue of Vinblastine † , ‡

ARTICLE *in* BIOCHEMISTRY · DECEMBER 2002

Impact Factor: 3.02 · DOI: 10.1021/bi026182m · Source: PubMed

Interaction of Tubulin with a New Fluorescent Analogue of Vinblastine[†,‡]

Sabarni K. Chatterjee,[§] Julien Laffray,[§] Pruthvi Patel,[§] Rudravajhala Ravindra,[§] Yong Qin,[||] Martin E. Kuehne,[||] and Susan L. Bane*[,§]

Department of Chemistry, State University of New York, Binghamton, New York 13902-6016, and Department of Chemistry, University of Vermont, Burlington, Vermont 05405

Received May 23, 2002; Revised Manuscript Received August 23, 2002

ABSTRACT: Vinblastine is an antimitotic agent that has been used extensively in cancer chemotherapy. The biological effects of the drug are believed to be the result of its interaction with tubulin, the major component of cellular microtubules. Fluorescence spectroscopy is a powerful and versatile technique for studying drug−tubulin interactions, but it rarely has been applied to studies involving vinca alkaloids. We have prepared a new fluorescent derivative of vinblastine designed to retain high affinity for tubulin while possessing a fluorophore that absorbs and emits visible light. A coumarin derivative of vinblastine, 17-deacetyl-*O*-(3-carbonylamino-7-diethylaminocoumarin) vinblastine (F-VLB), was prepared by reaction of 17-deacetylvinblastine with 7-diethylaminocoumarin-3-carbonyl azide. F-VLB was a potent inhibitor of in vitro microtubule assembly ($IC_{50} = 0.5\ \mu M$). F-VLB binding to tubulin was inhibited by vinblastine. Tubulin binding induced an increase in the F-VLB emission intensity and shifted the emission maximum to higher energy (from 500 to 480 nm). The Stokes shift of tubulin-bound F-VLB was about the same as the Stokes shift of the molecule in ethanol, indicating that the tubulin-bound fluorophore is probably on the exterior of the vinblastine binding site. Unlike vinblastine, F-VLB failed to induce self-assembly of tubulin that could be detected by light scattering or electron microscopy, although some self-association could be detected by analytical ultracentrifugation. Equilibrium binding parameters were quantitatively determined by monitoring the change in fluorescence anisotropy of F-VLB upon tubulin binding. The apparent equilibrium constant for F-VLB binding to tubulin [$K_a^{app} = (7.7 \pm 0.5) \times 10^4\ M^{-1}$ at 25 °C] was identical to the equilibrium constant for vinblastine binding to 2 μM tubulin (K_1) measured under similar buffer and temperature conditions using ultracentrifugation [Vulevic, B., Lobert, S., and Correia, J. J. (1997) *Biochemistry 36,* 12828−12835]. Binding allocolchicine to tubulin did not significantly affect F-VLB's affinity for the protein [$K_a^{app} = (9.1 \pm 0.4) \times 10^4\ M^{-1}$ at 25 °C]. Analysis of the steady-state emission spectra yielded a distance between the colchicine and vinca binding sites on tubulin of ∼40 Å. F-VLB bound to paclitaxel- and glutaraldehyde-stabilized microtubules, with approximately equal affinity. We conclude that F-VLB can be used to obtain information about the vinblastine binding site on tubulin under equilibrium conditions.

Vinca alkaloids have been used in cancer chemotherapy for more than 30 years. Several of these compounds have shown a broad spectrum of antitumor activity as single agents as well as in combination therapy (*1*). Vinblastine and its derivatives are believed to exert their therapeutic effects through interactions with tubulin, the major component of microtubules. At low concentrations, vinblastine inhibits tubulin assembly into microtubules and can depolymerize intact microtubules (*2*). At higher concentrations, vinblastine causes tubulin to assemble into spiral aggregates that can be detected by light scattering and eventually into paracrystals. Although all of these activities have been observed in cells, the activity most relevant to cytotoxicity may be the drug's effect on microtubule dynamics (*3*). At nanomolar concentrations, vinblastine, colchicine, and paclitaxel inhibit the rate and extent of microtubule shortening without significantly changing the polymer mass (*4*). The vinca alkaloids have an additional effect on microtubule ends not observed with other classes of antimicrotubule drugs, which is the induction of protofilament spirals. The spirals can be propagated into the microtubule, opening them in a spiraling fashion. The "spiraling potential" of these drugs has been correlated with cytotoxicity against L1210 cells, indicating that this parameter may also be relevant in the antitumor activity of vincas (*5*−*7*).

Despite the clinical importance of vincristine and vinblastine, the molecular features of the drug−receptor interaction are not well understood. The vinca alkaloid binding site on tubulin is distinct from the colchicine and paclitaxel binding sites on the protein, but the precise location of the site is currently unknown. Recent photoaffinity labeling results indicate that the binding site is on the β-subunit of tubulin (*8*), near the interdimer interface (*9*). Thermodynamic analyses have shown that the association between the vincas

[†] This work was supported by NIH Grants CA 69571 (S.L.B.) and CA R01-12010 (M.E.K.).

[‡] A portion of this work was presented at the 40th Annual Meeting of the American Society for Cell Biology, December 2000.

* To whom correspondence should be addressed. Telephone: (607) 777-2927. Fax: (607) 777-4478. E-mail: sbane@binghamton.edu.

[§] State University of New York.

[||] University of Vermont.

10.1021/bi026182m CCC: $22.00
Published on Web 11/01/2002

and tubulin is complex and highly dependent on solution variables (*10*). In most instances, tubulin binding is tightly linked to self-association of the protein.

Fluorescence spectroscopy is a powerful technique for studying ligand−receptor interactions and has been extensively used to study drug binding to the colchicine and paclitaxel binding sites on tubulin (*11*, *12*). Its use in studying the interactions of vinca alkaloids has been limited. Previously, only one fluorescent derivative of vinblastine had been synthesized and studied (*8*, *13*). This compound was ∼7-fold less potent than vinblastine as an inhibitor of tubulin assembly, and the quantum yield of the protein-bound drug was quite low. We report here the synthesis of a new fluorescent derivative of vinblastine that has a higher intrinsic fluorescence and can be excited with visible light. This compound retains high antimicrotubule activity, apparently mediated through its interaction with the vinblastine binding site on tubulin. The spectral properties of this fluorescent derivative of vinblastine make it a good candidate for use in fluorescence resonance energy transfer (FRET) studies and fluorescence microscopy.

MATERIALS AND METHODS

Materials. PIPES,[1] EGTA, and GTP (type II-S) were purchased from Sigma. Spectrograde solvents were used in absorption spectroscopy. The buffers that were used were as follows: PME buffer and PMEG buffer. Paclitaxel was obtained from David G. I. Kingston of Virginia Polytechnic and State University (Blacksburg, VA); allocolchicine was prepared as previously described (*14*). Vinblastine sulfate was a gift from Gideon Richter Ltd.

Synthesis of Fluorescent Vinblastine. A solution of 17-deacetylvinblastine (0.071 g, 0.092 mmol) and 7-diethylaminocoumarin-3-carbonyl azide (0.025 g, 0.084 mmol) in 1 mL of dry toluene was heated to 85 °C for 4 h. The reaction mixture was subjected to chromatography (20:1:1 ethyl acetate/methanol/triethylamine mixture) to afford 0.053 g (62.3%) of 17-deacetyl-*O*-(3-carbonylamino-7-diethylaminocoumarin) vinblastine: TLC $R_f = 0.30$ (silica plates, 20:1:1 ethyl acetate/methanol/triethylamine mixture); $[\alpha]^{25}_D = -62.5$ (*c* 0.4, CH_2Cl_2); UV (ethanol) λ_{max} 214, 262, 388 nm; IR ν_{max} 3468, 3399, 2968, 2935, 2878, 1738, 1703, 1612, 1523, 1459, 1432, 1409, 1371, 1358, 1333, 1302, 1244, 1130, 1035, 1009 cm^{-1}; ^1H NMR ($CDCl_3$) δ 8.31 (s, 1H), 8.04 (s, 1H), 7.52 (d, $J = 7.8$ Hz, 1H), 7.22 (d, $J = 10.8$ Hz, 1H), 7.20−7.08 (m, 4H), 6.63 (s, 1H), 6.61 (dd, $J = 2.4$, 9.8 Hz, 1H), 6.5 (d, $J = 2.3$ Hz, 1H), 6.12 (s, 1H), 5.88 (dd, $J = 3.8$, 10.3 Hz, 1H), 5.46 (s, 1H), 5.44 (d, $J = 10.4$ Hz, 1H), 3.96 (t, $J = 7.4$ Hz, 1H), 3.85−3.72 (m, 2H), 3.79 (s, 6H), 3.74 (s, 1H), 3.62 (s, 3H), 3.45−3.22 (m, 10H), 3.15 (m, 2H), 3.03 (m, 1H), 2.90−2.80 (m, 4H), 2.73 (s, 3H), 2.69 (s, 1H), 2.45 (m, 2H), 2.29 (dd, $J = 2.9$, 9.5 Hz), 2.15 (m, 1H), 2.84 (m, 2H), 1.50−1.25 (m, 9H), 1.21 (t, $J = 7.1$ Hz, 6H), 0.98−0.85 (m, 1H), 0.89 (t, $J = 7.5$ Hz, 3H), 0.84 (t, $J = 7.4$ Hz, 3H); low-resolution mass spectrum (FAB) 1027 (M + 1); high-resolution mass spectrum (FAB), calcd for $C_{58}H_{71}N_6O_{11}$ 1027.5184 (M + 1), found 1027.5151.

Tubulin Purification and Protein Determination. Microtubule protein (MTP) and tubulin were prepared by two cycles of assembly and disassembly as described by Williams and Lee (*15*). The protein solution at the end of the second cycle was drop-frozen into liquid nitrogen to yield MTP or was subjected to phosphocellulose chromatography to yield pure tubulin, which was also drop-frozen into liquid nitrogen. Prior to use, the frozen protein pellets were gently thawed, centrifuged at 1000*g* for 10 min at 4 °C, and then desalted into the appropriate buffer on 1 mL Sephadex G-50 columns.

Tubulin concentrations were determined spectrophotometrically using an extinction coefficient of 1.23 $(mg/ml)^{-1}$ cm^{-1} at 278 nm in PME buffer (*16*). The concentrations of fluorescent vinblastine and vinblastine were also determined spectrophotometrically using extinction coefficients determined in our lab: $\epsilon_{390} = 2.35 \times 10^4$ M^{-1} cm^{-1} for F-VLB in DMSO and $\epsilon_{292} = 1.54 \times 10^4$ M^{-1} cm^{-1} for vinblastine in DMSO.

Preparation of Tubulin-Bound Allocolchicine. Tubulin-bound allocolchicine was prepared by incubating tubulin with a 10-fold excess of allocolchicine at 37 °C for 30 min in PME buffer. Excess allocolchicine was removed by the rapid gel filtration method of Penefsky (*17*). The sample was stored at 4 °C until it was used.

Preparation of Stabilized Microtubules. Tubulin (50 μM) was assembled into microtubules in PG buffer at 37 °C and then cross-linked with 20 mM glutaraldehyde as described by Andreu et al. (*18*). The cross-linked microtubules were stored at 4 °C for up to 1 week. Paclitaxel-stabilized microtubules were freshly prepared by inducing tubulin (in PMEG buffer) polymerization with a 2-fold excess of paclitaxel at 37 °C for 30 min.

Microtubule Assembly Assay. Assembly of MTP was monitored turbidimetrically using a Hewlett-Packard model 8453 absorption spectrophotometer with a thermostated multicell holder maintained at 37 °C. The basic experimental protocol was as follows. MTP (1 mg/mL) in PME buffer was equilibrated with varying concentrations of F-VLB in DMSO in the sample cell, and a baseline was recorded. The final concentration of DMSO was always <4% of the total volume. Assembly was initiated by adding GTP to a final concentration of 1 mM. The apparent absorption at 350 nm was recorded at 30 s intervals until a steady state was reached. The extent of polymerization was determined by the difference in the initial and saturation absorption values. The IC_{50} was calculated from the linear part of a graph of percent inhibition versus F-VLB concentration.

Steady-State Fluorescence Spectroscopy. Fluorescence emission spectra for tubulin−F-VLB ($\lambda_{ex} = 390$ nm) and tubulin allocolchicine−F-VLB ($\lambda_{ex} = 310$ nm) complexes were recorded using an SLM 48000s spectrofluorometer or a Spex FluoroMax-3 spectrofluorometer. Fluorescence anisotropy measurements were performed in the FluoroMax-3 instrument in the polarization mode ($\lambda_{ex} = 390$ nm, $\lambda_{em} = 490$ nm).

Equilibrium constants were determined by fluorescence anisotropy titrations. F-VLB (0.25 μM) in PMEG buffer was incubated with tubulin (0−16 μM) or tubulin-bound allo-

[1] Abbreviations: MTP, microtubule protein; GTP, guanosine 5′-triphosphate; GDP, guanosine 5′-diphosphate; DMSO, dimethyl sulfoxide; EGTA, ethylene glycol bis(β-aminoethyl ether)-*N*,*N*,*N*′,*N*′-tetraacetic acid; PIPES, piperazine-*N*,*N*′-bis(2-ethanesulfonic acid); PME buffer, 100 mM PIPES, 1 mM $MgSO_4$, and 2 mM EGTA (pH 6.9); PMEG buffer, PME buffer containing 0.1 mM GTP (pH 6.9); PG buffer, 10 mM sodium phosphate, 1 mM EGTA, 0.1 mM GTP, and 3.5 M glycerol (pH 6.8); F-VLB, 17-deacetyl-*O*-(3-carbonylamino-7-diethylaminocoumarin) vinblastine.

colchicine (0−35 μM) at 25 °C for 5 min, and the anisotropy of F-VLB in each solution was measured. The apparent association constant (K_a) was determined using the equation

$$\alpha = n[\mathrm{Tb}]_{\mathrm{free}}/(K_d + [\mathrm{Tb}]_{\mathrm{free}})$$

where α is the fraction of F-VLB bound with tubulin. This parameter is calculated by $(R - R_0)/(R_{max} - R_0)$, where R is the anisotropy of F-VLB in the presence of tubulin, R_0 is the anisotropy of F-VLB in the absence of tubulin, R_{max} is the anisotropy of F-VLB fully bound to tubulin, and K_d is the apparent dissociation constant and is equal to the reciprocal of the apparent association constant. $[\mathrm{Tb}]_{\mathrm{free}}$ was calculated by

$$[\mathrm{Tb}]_{\mathrm{free}} = [\mathrm{Tb}]_0 - \alpha[\mathrm{F\text{-}VLB}]_0$$

where $[\mathrm{Tb}]_0$ is the total concentration of tubulin and $[\mathrm{F\text{-}VLB}]_0$ is the total concentration of F-VLB. The number of F-VLB binding sites on tubulin (n) is unity in these analyses, since the concentration of bound drug is determined from a ratio of spectroscopic signals.

The above equation assumes that the fluorescence intensity of the ligand is unchanged with receptor binding (*19*). Since the emission intensity of F-VLB increased upon tubulin binding, it was necessary to correct the fraction bound for the intensity difference. This was done by the method of Lundblad (*20*) using the following equation:

$$\alpha_{corr} = (R - R_0)/[(R_{max} - R)(Q_b/Q_f) + R - R_0]$$

where α_{corr} is the fraction of tubulin-bound ligand corrected for the fluorescence intensity change due to receptor binding, Q_f is the fluorescence intensity of F-VLB (λ_{ex} = 390 nm, λ_{em} = 490 nm) in the absence of tubulin, and Q_b is the fluorescence intensity of F-VLB (λ_{ex} = 390 nm, λ_{em} = 490 nm) at saturating concentrations of tubulin.

Competition of F-VLB Binding to Tubulin by Vinblastine. A fluorescence anisotropy-based competition assay between F-VLB and vinblastine binding to tubulin was performed. F-VLB (1 μM) and tubulin (10 μM) in PME buffer at 25 °C were titrated with excess vinblastine. The anisotropy of F-VLB in each of the samples was measured. The percentage of F-VLB bound in each sample was determined as a fraction of the anisotropy value of the sample containing no vinblastine. The IC_{50} (50% inhibitory concentration) was calculated from a plot of the percentage of F-VLB bound versus vinblastine concentration. An inhibition constant (K_i) for vinblastine was determined by using the method of Cheng and Prussoff (*21*):

$$K_i = IC_{50}/(1 + [\mathrm{F\text{-}VLB}]/K_d)$$

where K_d is the dissociation constant for F-VLB binding to tubulin.

Determination of the Förster Distance for Tubulin-Bound Allocolchicine and F-VLB. The Förster distance (R_0, in angstroms), which is the distance at which energy transfer is 50% efficient, was determined with the following equation:

$$R_0 = 0.211[\kappa^2 \eta^{-4} Q_D J(\lambda)]^{1/6}$$

where $J(\lambda)$ is the overlap integral between the donor (allocolchicine) fluorescence emission spectrum and the acceptor (F-VLB) absorption spectrum, κ^2 is the orientation factor, Q_D is the quantum yield of the donor in the absence of the acceptor, and η is the refractive index (*19*). The spectral overlap integral, $J(\lambda)$, was calculated by numerical integration; κ^2 was assumed to be $^2/_3$ (*19*). The refractive index (η) of water (1.33) was used for the calculation. The quantum yield of allocolchicine bound to tubulin is 0.29 (*22*).

Estimation of the Interfluorophore Distance for Tubulin-Bound Allocolchicine and F-VLB. The distance between F-VLB and allocolchicine bound to tubulin was estimated from the steady-state emission spectra of the donor (allocolchicine) as described in ref *19*, using the data from Figure 7. The intensity of emission of 5 μM tubulin-bound allocolchicine (D) and of 5 μM tubulin-bound allocolchicine in the presence of 12 μM F-VLB (DA) in PMEG buffer was measured at 390 nm in a 2 mm × 10 mm fluorescence cell, oriented such that the excitation beam passed through the short path. The emission intensity of DA at 390 nm was corrected for inner filter effects as described in ref *19* using the equation

$$F_{corr} = F_{obs}\ \mathrm{antilog}\left(\frac{OD_{ex} + OD_{em}}{2}\right)$$

where F_{obs} is the observed emission intensity of DA, F_{corr} is the emission intensity corrected for inner filter effects, OD_{ex} is the absorption of the DA solution at the excitation wavelength divided by 5 to account for the short path for the excitation beam, and OD_{em} is the absorption of the DA solution at the emission wavelength. The corrected intensity was used to calculate the energy transfer efficiency (E), which must then be corrected for incomplete labeling of the acceptor using

$$E = \left(1 - \frac{F_{DA}}{F_D}\right)\frac{1}{f_A}$$

where F_D and F_{DA} are the emission intensities of the donor in the absence and presence of acceptor, respectively, and f_A is the fraction of the receptor with bound acceptor. The fraction of tubulin-bound allocolchicine bound to F-VLB was calculated from the dissociation constant assuming a single ligand binding site. Finally, this value for efficiency was used to calculate the interfluorophore distance using

$$E = \frac{R_o^6}{R_o^6 + r^6}$$

where r is the D−A distance.

Electron Microscopy. Single drops of the assembled tubulin solutions containing F-VLB were placed on 200 mesh hydrophilic carbon-coated grids for 1 min. The excess solution was removed with filter paper. The grid was rinsed with 100 mM ammonium acetate and was negatively stained by application of 1% (w/v) aqueous uranyl acetate for 1 min. Samples were observed with a Hitachi 7000 TEM electron microscope operated at 100 kV.

RESULTS

Synthesis of F-VLB. Rai and Wolff prepared a fluorescent derivative of vinblastine in which an *o*-aminobenzoate

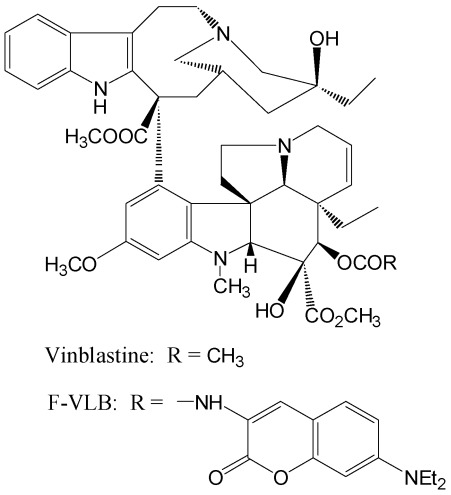

FIGURE 1: Structures of vinblastine and F-VLB.

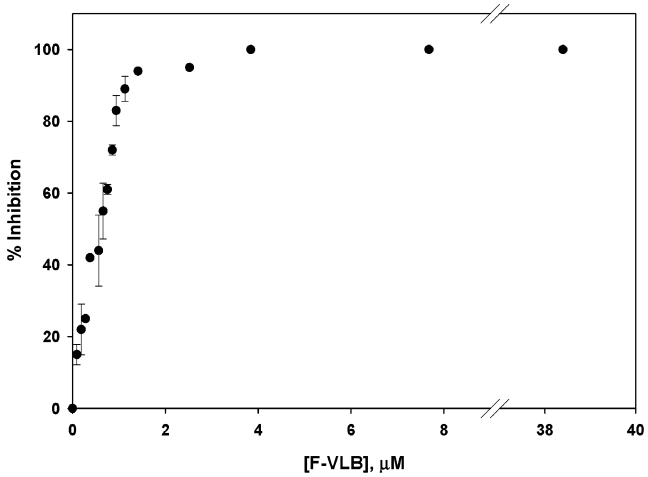

FIGURE 2: Effect of F-VLB on the assembly of microtubule protein. Microtubule protein (1 mg/mL) was treated with varying concentrations of F-VLB and incubated at 37 °C for 15 min. GTP was added to a final concentration of 1 mM to initiate polymerization. Assembly was monitored by the apparent absorption at 350 nm. The percent inhibition was calculated from absorption values after a steady state had been reached.

fluorophore was attached to the C-20′ alcohol (*8*). We attempted to prepare a coumarin-labeled derivative of vinblastine using similar chemistry but were unsuccessful. Mechanistic and spectroscopic studies with purified tubulin indicate that the vindoline portions of the vincas serve as an anchor, while the cleavamine portions of the molecules induce most of the drugs' effects on tubulin (*23*, *24*). We therefore hypothesized that a fluorophore attached to the vindoline portion of vinblastine might not affect the drug−tubulin interaction and chose the 17 position on the vindoline as an alternate location for a fluorophore. F-VLB (Figure 1) was prepared in a 62% yield by reaction of 17-deacetylvinblastine with 7-diethylaminocoumarin-3-carbonyl azide.

Inhibition of in Vitro Microtubule Assembly by F-VLB. The first task was to determine whether the appended fluorophore affected the activity of the vinblastine derivative. The effect of F-VLB on the assembly of microtubule protein (MTP) is shown in Figure 2. Assembly was inhibited by 50% at an F-VLB concentration of 0.5 μM, and complete inhibition was observed at 3 μM F-VLB. Virtually identical behavior was observed for vinblastine at low concentrations

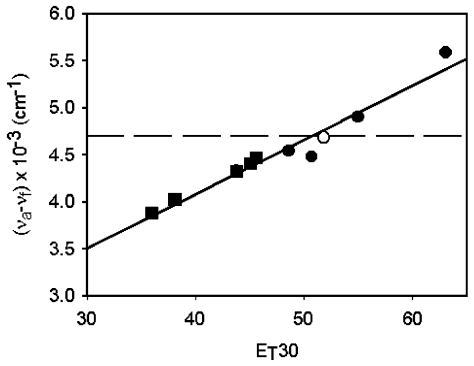

FIGURE 3: Effect of solvent on the Stokes shift of F-VLB. The squares are aprotic solvents (from left to right, dioxane, ethyl acetate, dimethylformamide, dimethyl sulfoxide, and acetonitrile). The circles are protic solvents (from left to right, 2-propanol, 1-propanol, ethanol, methanol, and water). The dashed line is the Stokes shift of F-VLB bound to tubulin, which is approximately the same value as the Stokes shift of F-VLB in ethanol (○). E_T30 is an empirical solvent polarity parameter (*19*).

(data not shown), indicating that the fluorophore does not affect the inhibitory activity of the parent molecule. In contrast to vinblastine, however, F-VLB did not appear to induce tubulin aggregation that could be detected by light scattering, even at high concentrations. Electron micrographs of F-VLB (up to 500 μM) with 1 mg/mL MTP showed no significant aggregation or spiral formation, which is typical for vinblastine-like drugs (*25*).

Spectroscopic Properties of F-VLB. The absorption and emission spectra of F-VLB were recorded in a variety of solvents. The dependency of the Stokes shift on the solvent polarity was essentially linear, although a slight increase in the slope was evident in protic solvents (Figure 3). The photochemical properties of the fluorescent probe in F-VLB can therefore be described by simple solvent effects (*19*). The absorption and emission spectra of F-VLB in buffer and in the presence of tubulin are shown in Figure 4. The absorption spectrum of F-VLB exhibits a low-energy band corresponding to the coumarin moiety, which is well separated from the absorption bands of vinblastine itself (Figure 4A). Tubulin binding caused an 8−10-fold increase in emission intensity and a shift of the emission maximum to higher energy (Figure 4B). The Stokes shift of tubulin-bound F-VLB is indicated by the dashed line in Figure 3. The Stokes shift of the tubulin-bound species was very similar to the Stokes shift of the molecule in ethanol [Figure 3 (○)]. Thus, the fluorophore in F-VLB bound to tubulin is in a quite polar environment, indicating that the fluorophore is likely to be on the exterior of the ligand binding site.

Direct Measurements of the Level of F-VLB Binding to Tubulin. The association of F-VLB with tubulin was quantitatively assessed by monitoring the change in fluorescence anisotropy of a fixed concentration of F-VLB in the presence of increasing concentrations of tubulin. A plateau in the anisotropy change was reached at a molar ratio of tubulin to F-VLB of ∼30:1 (Figure 5A). Since the fluorescence of F-VLB also increased upon tubulin binding, it was necessary to correct the fraction bound calculated from the anisotropy data for the emission intensity change (*19*). The corrected binding data, calculated as described in Materials and Methods, were fit to a singular rectangular hyperbola [Figure 5A (■)]. Nonlinear regression analysis of

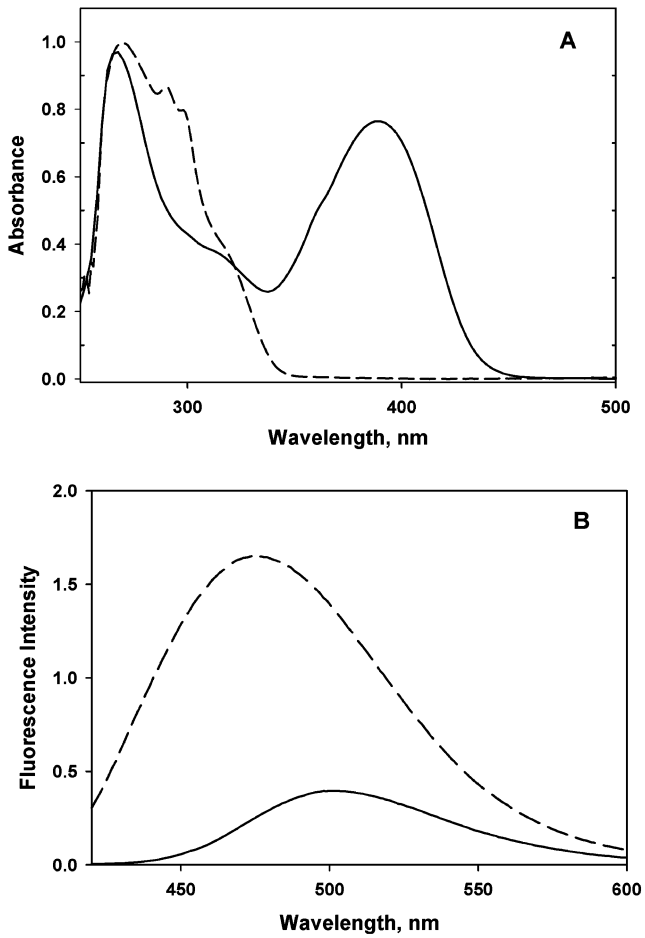

FIGURE 4: Spectral properties of F-VLB. (A) The absorption spectrum of 8 μM F-VLB (—) and 55 μM vinblastine (– – –) in DMSO. (B) The emission spectra of 1 μM F-VLB in PMEG buffer in the absence (—) and presence (– – –) of 15 μM tubulin. The excitation wavelength was 390 nm, and the temperature was 25 °C.

the corrected data yielded an apparent association constant of $(7.7 \pm 0.5) \times 10^4$ M^{-1} at 25 °C.

The increase in F-VLB emission intensity upon tubulin binding could also be employed to measure binding constants. If a fixed concentration of tubulin was titrated with increasing concentrations of F-VLB, however, corrections for inner filter effects and for the fluorescence of unbound ligand were more unwieldy than correcting the anisotropy data. Moreover, tubulin aggregation is more likely when the vinblastine derivative rather than the protein is in excess. When a fixed concentration of F-VLB was titrated with tubulin, the apparent association constant determined by monitoring emission intensity was within experimental error of the association constant measured using fluorescence anisotropy.

We intend to use F-VLB to perform distance measurements between ligand binding sites on tubulin, so it was important to assess the affinity of the probe for tubulin bound to other drugs. Allocolchicine possesses suitable spectral overlap with F-VLB to serve as an energy transfer donor for the colchicine site (Figure 6). The association of F-VLB with the allocolchicine−tubulin complex was analyzed in the same manner as the association of F-VLB with tubulin (Figure 5B), yielding a slightly larger association constant

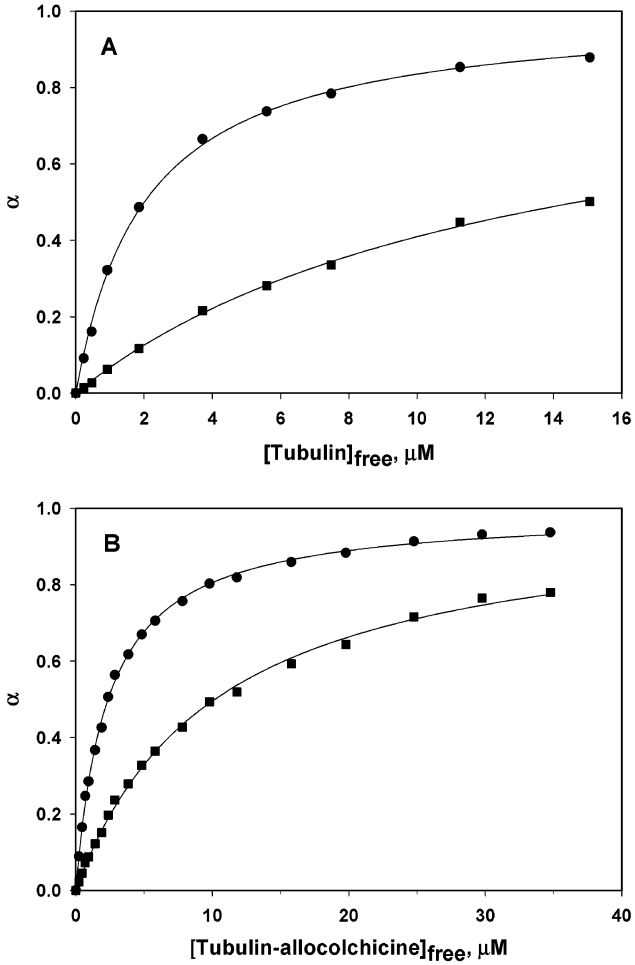

FIGURE 5: Equilibrium binding of F-VLB to tubulin and the tubulin−allocolchicine complex in PMEG buffer. The binding of F-VLB to tubulin (A) and the tubulin−allocolchicine complex (B) was monitored by the change in the fluorescence anisotropy of 0.25 μM F-VLB as a function of tubulin concentration (λ_{ex} = 390 nm, λ_{em} = 490 nm). The values of fraction bound (α) calculated from the raw anisotropy data (●) were corrected (■) for the difference in emission intensity of the free and bound ligand as described in Materials and Methods. The temperature was maintained at 25 °C.

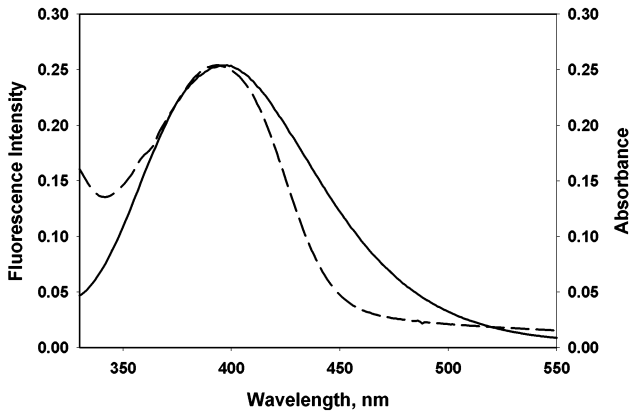

FIGURE 6: Spectral overlap of allocolchicine and F-VLB. The spectral overlap between the emission (λ_{ex} = 310 nm) of the donor (5 μM allocolchicine) in the presence of 5 μM tubulin (—) and the absorption spectrum of the acceptor (5 μM F-VLB) in the presence of 5 μM tubulin (– – –) is illustrated. An R_0 of 33 Å was calculated for the donor−acceptor pair.

[$(9.1 \pm 0.4) \times 10^4$ M^{-1} at 25 °C]. Simultaneous tubulin binding of both allocolchicine and F-VLB resulted in a decrease in the emission intensity of tubulin-bound allo-

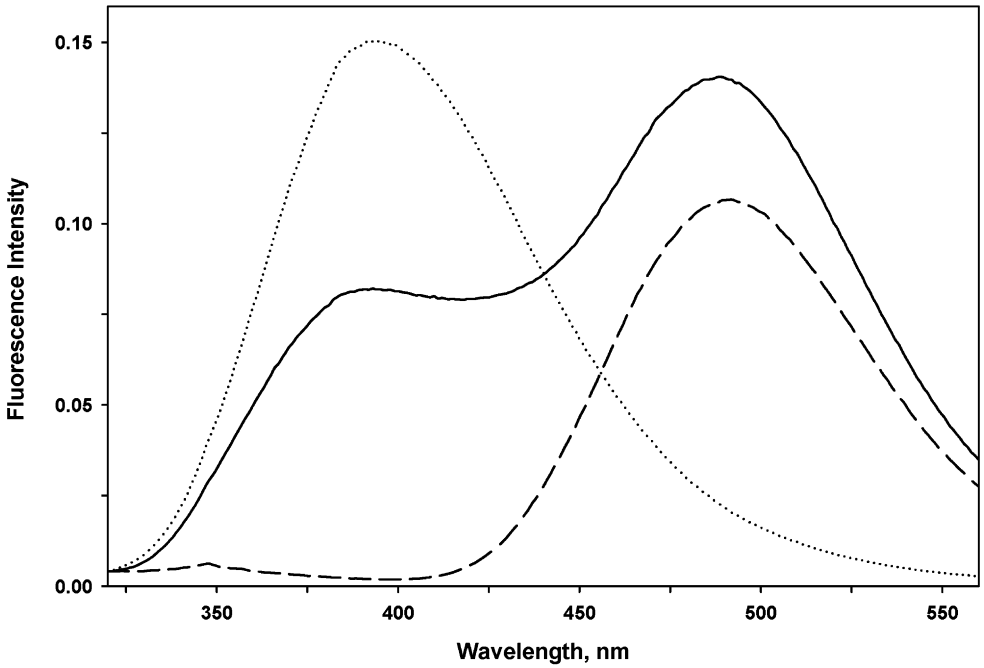

FIGURE 7: Energy transfer from tubulin-bound allocolchicine to tubulin-bound F-VLB. The solid curve is the emission spectrum of the allocolchicine−tubulin complex (5 μM) in the presence of 12 μM F-VLB in PMEG buffer, excited in the allocolchicine absorption band (310 nm). The dotted curve is the emission spectrum of the allocolchicine−tubulin complex (5 μM) in PMEG buffer (λ_{ex} = 310 nm). The dashed curve is the emission spectrum 12 μM F-VLB in PMEG buffer (λ_{ex} = 310 nm). The efficiency of energy transfer was calculated from the emission intensity of the donor (allocolchicine−tubulin complex) at 390 nm in the absence and presence of F-VLB as described in Experimental Procedures. The temperature was 25 °C.

colchicine and a concomitant increase in the emission intensity of tubulin-bound F-VLB (Figure 7), indicating that energy transfer between allocolchicine and F-VLB does occur. The distance between the two fluorophores was calculated from the emission spectrum of the donor. Calculation of the distance using the emission spectrum of the donor for these data requires corrections for secondary absorption effects and for incomplete acceptor labeling as described in Materials and Methods (*19*). A value of 40 Å for the interfluorophore distance was obtained after the appropriate corrections were applied.

The binding of F-VLB to tubulin was inhibited by excess vinblastine, supporting our hypothesis that F-VLB and vinblastine bind to the same site on tubulin (Figure 8). An apparent inhibition constant (K_i) of 32 μM was calculated. It must be noted that this analysis did not take into account vinblastine-induced tubulin association, which may affect the value of the inhibition constant (*26*). Moreover, since the level of tubulin-bound F-VLB was monitored using fluorescence anisotropy, there were more vinblastine binding sites than molecules of F-VLB in all samples. The apparent inhibition constant is therefore a high estimate of the true inhibition constant.

Direct Measurements of the Level of F-VLB Binding to Microtubules. We hope to use F-VLB as an energy transfer acceptor for fluorescent paclitaxels previously studied in our lab (*27*, *28*), so we sought to assess the affinity of F-VLB for intact microtubules. We first attempted to evaluate the binding of F-VLB to paclitaxel-induced microtubules. The fluorescence anisotropy of F-VLB was measured with increasing concentrations of paclitaxel-induced microtubules, and a normal saturation curve was observed (Figure 9). A similar curve was produced when the F-VLB emission intensity was used as the spectroscopic signal (data not shown). Electron microscopy of the paclitaxel-induced microtubules (5 μM) in the presence of low concentrations of F-VLB (1 μM) showed mostly irregular sheets and few normal microtubules (data not shown). We therefore prepared what should be more stable microtubules, glycerol-induced microtubules cross-linked with glutaraldehyde (*18*). The anisotropy titration curve for F-VLB binding to glutaraldehyde-stabilized microtubules was very similar to the curve for F-VLB binding to paclitaxel-induced microtubules (Figure 9). Electron microscopy of these microtubules (5 μM) in the presence of 1 μM F-VLB showed mostly microtubules, but also a significant number of spiral ribbons (Figure 10).

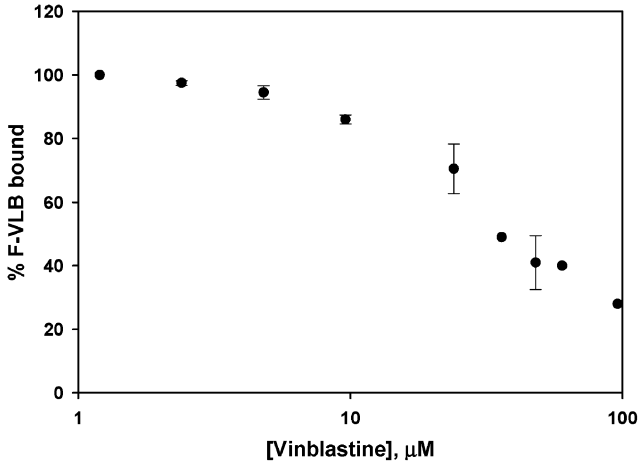

FIGURE 8: Inhibition of F-VLB binding to tubulin by vinblastine. Tubulin bound to F-VLB was prepared by incubating tubulin (10 μM) and F-VLB (1 μM) for 15 min at 25 °C. The anisotropy of F-VLB was measured (λ_{ex} = 390 nm, λ_{em} = 490 nm) using varying concentrations of vinblastine at 25 °C.

The binding curves for F-VLB binding to tubulin polymers (Figure 9) were very similar to the curves for F-VLB binding

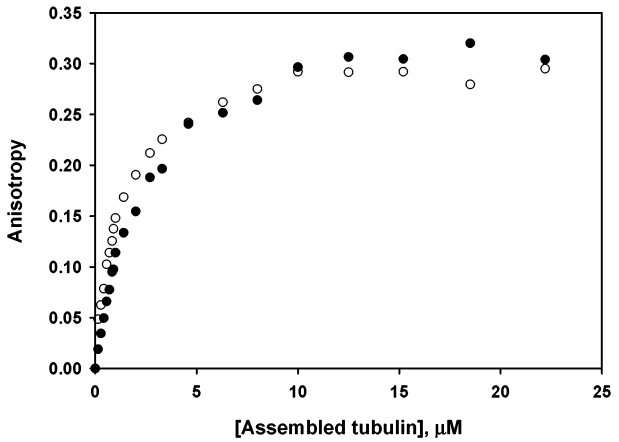

FIGURE 9: Binding of F-VLB to microtubules. The binding of F-VLB to microtubules was monitored by recording the anisotropy of F-VLB (0.25 μM) in the appropriate buffer with increasing concentrations of microtubules (λ_{ex} = 390 nm, λ_{em} = 490 nm): (○) paclitaxel-induced microtubules and (●) glutaraldehyde-stabilized microtubules. The concentration of the polymer is estimated from the concentration of tubulin dimers in solution prior to assembly. The temperature was maintained at 25 °C.

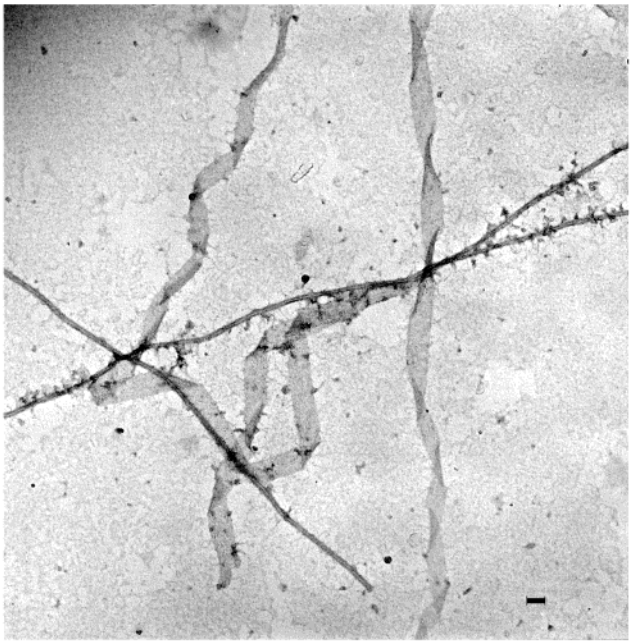

FIGURE 10: Electron micrograph of cross-linked microtubules (5 μM) in the presence of 1 μM F-VLB. The bar is 0.1 μm.

to unassembled tubulin or the tubulin−allocolchicine complex (data not shown). If all of the tubulin dimers in the solutions of paclitaxel- or glutaraldehyde-bound microtubules are capable of binding fluorescent vinblastine, then the apparent association constant for vinblastine binding to the protein in the polymer solution will be approximately the same as the apparent association constant for vinblastine binding to unassembled tubulin.

DISCUSSION

The association of vincristine and vinblastine with tubulin was first investigated more than 20 years ago (*29*). It was clear that the ligand−receptor interaction was not a straightforward association; different laboratories reported different conclusions about the number of binding sites on tubulin and the affinity of the drug for the binding site(s) (*30*). Timasheff and co-workers demonstrated that the binding of vincristine and vinblastine to tubulin is tightly linked to self-association of the protein and therefore cannot be analyzed by simple isotherms (*31*). The overall reaction of vinblastine with tubulin is best described by a ligand-mediated plus ligand-facilitated isodesmic self-association (*9*). Lobert and Correia have demonstrated that the overall process is also dependent on the chemical nature of the nucleotide bound to tubulin, the concentration of magnesium ion, and the ionic strength of the buffer solution (*6*, *32*). Comparison of quantitative data from different reports must therefore take into account these parameters.

Fluorescence spectroscopy is a powerful and versatile tool for probing ligand−receptor interactions. With an appropriate fluorophore, assessments of ligand−receptor interactions can be performed without disrupting equilibrium conditions. Ideally, the appended fluorophore does not affect the ligand−receptor interaction; this is, however, rarely the case. In this study, we sought to examine the vinblastine−tubulin association using fluorescence spectroscopy. We chose to attach an environmentally sensitive fluorphore to the vindoline portion of vinblastine, which we hoped would not adversely affect the interaction of the molecule with its receptor. We found that this fluorescent derivative of vinblastine, termed F-VLB, acted like vinblastine in several important ways. F-VLB was equipotent with vinblastine as an inhibitor of microtubule assembly, and the binding of F-VLB to tubulin was inhibited by vinblastine. There was, however, a major difference between the tubulin binding properties of F-VLB and vinblastine. We could find no evidence by light scattering or by electron microscopy that F-VLB causes tubulin to self-associate.

In the absence of tubulin self-association, the equilibrium binding data may be analyzed as a single ligand−receptor binding process, yielding an apparent equilibrium constant for F-VLB binding to tubulin. It cannot be concluded, however, that F-VLB does *not* induce self-association of tubulin. The two techniques at our disposal are not suitable for detecting small oligomers that may be present in the solutions. Moreover, vinca-induced self-association is highly dependent on ligand and protein concentrations (*26*). Tubulin was in large molar excess over F-VLB in most of our analyses. Under these conditions, vinblastine-induced self-assembly is not usually observed (*7*).

The difference between the tubulin binding activities and tubulin self-association activities of F-VLB is not unprecedented. Lobert et al. (*7*) have shown that structural variations in a large series of vinca alkaloids have little effect on the affinity of the molecule for tubulin heterodimers, which they term K_1. In the same series of compounds, however, the affinity of liganded tubulin for the growing tubulin polymer (K_2) differs by a factor of as much as 100. The apparent equilibrium constant measured here for F-VLB binding to tubulin [K_a^{app} = (7.7 ± 0.5) × 10^4 M^{-1} at 25 °C] was identical to the equilibrium constant for vinblastine binding to 2 μM tubulin [K_1 = (8.4 ± 0.2) × 10^4 M^{-1}] measured under similar buffer and temperature conditions (*10*). Therefore, if F-VLB induces tubulin self-association, it does so weakly. In support of this interpretation of the data, it has been observed that F-VBL increases the average sedimentation coefficient of tubulin to a small extent (J. J. Correia, personal communication). Since the other tubulin binding

properties of F-VLB are very similar to those of vinblastine binding to tubulin, we submit that F-VLB is a suitable probe for the vinca alkaloid binding site on tubulin.

Tubulin binding induced a 20 nm blue shift in the emission spectrum of F-VLB and an 8−10-fold increase in emission intensity. The small changes in the energy and intensity of emission indicate that the fluorophore of F-VLB is on the exterior of the vinblastine binding site, which is consistent with expectations based on structure−activity studies (*24*). Tubulin binding also induced an increase in the fluorescence anisotropy of F-VLB, which was monitored to determine equilibrium constants for the association of F-VLB with tubulin and the allocolchicine−tubulin complex and to examine F-VLB binding to paclitaxel- and glutaraldehyde-stabilized microtubules.

We found that tubulin containing allocolchicine in the colchicine binding site had a slightly greater affinity for F-VLB than unliganded tubulin. The spectral overlap of the allocolchicine emission spectrum and the F-VLB absorption spectrum made the two ligands a suitable donor−acceptor pair for FRET. The excitation and emission spectra of F-VLB bound to the allocolchicine−tubulin complex showed a decrease in the allocolchicine emission intensity coupled with an increase in the F-VLB emission intensity (Figure 7), which is one characteristic of FRET (*19*). Calculation of a distance from these steady-state spectra required corrections for secondary absorption effects and incomplete receptor labeling. These calculations also assume that a single donor−acceptor pair is responsible for the spectral changes. This latter assumption may not be true if self-association of the liganded protein is present, which is a possibility that we cannot rule out. Time-resolved techniques will be required to determine whether the emission intensity changes are indeed due to a single event, which is beyond the scope of this report. Nevertheless, an estimate of the interfluorophore distance (∼40 Å) could be made from steady-state data. The vinca alkaloid binding site on tubulin has been suggested to be on the end of the microtubule (*32*), and the peptide identified by photoaffinity labeling is also in the vicinity of the exchangeable GTP binding site (*8*). The estimated distance from FRET analysis is in agreement with the vinblastine binding site being in the vicinity of the exchangeable GTP binding site.

Singer et al. (*34*) reported that vinblastine binds to paclitaxel-stabilized microtubules with an affinity 10-fold lower than its affinity for tubulin and a stoichiometry near 1.5 sites per mole of polymerized tubulin. We also observed F-VLB binding to stabilized microtubules; however, the association led to significant changes in the morphology of the microtubules, even at substoichiometric concentrations of F-VLB. Clearly, F-VLB binding induces a conformational change in the protein significant enough to overcome the stabilizing effects of paclitaxel and even chemical cross-links. The ribbons seen with cross-linked microtubules are reminiscent of the peeling spiral protofilaments formed by the action of vinblastine on microtubules (*35*). This observation supports the notion that F-VLB can indeed induce tubulin spiraling.

Interestingly, the binding curves for F-VLB associating with the tubulin polymers very closely resembled each other and the binding curves for F-VLB binding to unassembled tubulin. If it is assumed that all tubulin in the solution is capable of binding F-VLB, regardless of its assembly state, then the apparent association constants calculated for F-VLB binding to these systems would be approximately the same as the apparent association constants for F-VLB binding to tubulin and to the tubulin−allocolchicine complex. On the surface, this observation seems to oppose the conclusion of Wilson et al. (*32*), who found that vinblastine binds to the walls of microtubules with lower affinity than it binds to the ends. This is not necessarily the case. It is reasonable to hypothesize that vinblastine binding to microtubule walls is governed by K_1, the intrinsic affinity of vinblastine for tubulin, and the affinity of vinblastine for the ends of the microtubule is affected by both K_1 and K_2, the affinity of liganded tubulin for the growing tubulin polymer. Since K_2 appears to be quite small for F-VLB, microtubule ends and microtubule walls should bind F-VLB with the same apparent affinity, approximated by K_1.

Conclusions. A new fluorescent derivative of vinblastine has been prepared. Addition of a diethylaminocoumarin to the vindoline portion of vinblastine gives a molecule whose in vitro activity differs from that of vinblastine only in its ability to induce self-assembly of tubulin. F-VLB binding to tubulin is accompanied by an increase in ligand fluorescence emission intensity and fluorescence anisotropy, which can be used to quantitatively determine equilibrium binding parameters with tubulin and microtubules. Allocolchicine and F-VLB can simultaneously bind to tubulin and are a suitable donor and acceptor, respectively, for measurements of FRET. Analysis of steady-state data yields ∼40 Å between the colchicine and vinca alkaloid binding sites on tubulin, which is in good agreement with other experimental data. F-VLB also binds to paclitaxel-induced microtubules and to glutaraldehyde-cross-linked microtubules, and may therefore also serve as an energy transfer acceptor for a fluorescent probe in the paclitaxel binding site.

ACKNOWLEDGMENT

We thank Mr. Henry Eichelberger for assistance in obtaining the electron micrographs. We are grateful to Dr. John J. Correia of the University of Mississippi Medical Center Analytical Ultracentrifuge Facility (Oxford, MS) for providing the results of the ultracentrifuge analysis and for helpful suggestions for the manuscript.

REFERENCES

1. Rowinsky, E. K., and Donehower, R. C. (1991) *Pharmacol. Ther. 52*, 35−84.
2. Himes, R. H. (1991) *Pharmacol. Ther. 52*, 257−267.
3. Jordan, M. A., and Wilson, L. (1990) *Biochemistry 29*, 2730−2739.
4. Wilson, L., and Jordan, M. A. (1995) *Chem. Biol. 2*, 569−573.
5. Lobert, S., Ingram, J. W., Hill, B. T., and Correia, J. J. (1998) *Mol. Pharmacol. 53*, 908−915.
6. Lobert, S., Vulevic, B., and Correia, J. J. (1996) *Biochemistry 35*, 6806−6814.
7. Lobert, S., Fahy, J., Hill, B. T., Duflos, A., Etievant, C., and Correia, J. J. (2000) *Biochemistry 39*, 12053−12062.
8. Rai, S. S., and Wolff, J. (1996) *J. Biol. Chem. 271*, 14707−14711.
9. Correia, J. J., and Lobert, S. (2001) *Curr. Pharm. Des. 7*, 1213−1228.
10. Vulevic, B., Lobert, S., and Correia, J. J. (1997) *Biochemistry 36*, 12828−12835.
11. Andreu, J. M., Gorbunoff, M. J., Lee, J. C., and Timasheff, S. N. (1984) *Biochemistry 23*, 1742−1752.

12. Sengupta, S., Boge, T. C., Georg, G. I., and Himes, R. H. (1995) *Biochemistry 34*, 11889−11894.
13. Rai, S. S., and Wolff, J. (1997) *FEBS Lett. 416*, 251−253.
14. Fernholz, H. (1950) *Justus Liebigs Ann. Chem. 568*, 63−72.
15. Williams, R. C., Jr., and Lee, J. C. (1982) *Methods Enzymol. 85*, 376−385.
16. Detrich, H. W., III, and Williams, R. C., Jr. (1978) *Biochemistry 17*, 3900−3907.
17. Penefsky, H. S. (1979) *Methods Enzymol. 56*, 527−530.
18. Andreu, J. M., and Barasoain, I. (2001) *Biochemistry 40*, 11975−11984.
19. Lakowicz, J. R. (1999) *Principles of Fluorescence Spectroscopy*, 2nd ed., Plenum Publishers, New York.
20. Lundblad, J. R., Laurance, M., and Goodman, R. H. (1996) *Mol. Endocrinol. 10*, 607−612.
21. Cheung, Y. C., and Prusoff, W. H. (1973) *Biochem. Pharmacol. 22*, 3099−3108.
22. Hastie, S. B. (1989) *Biochemistry 28*, 7753−7760.
23. Gaggelli, E., Gaggelli, N., Maccotta, A., and Valensin, G. (1994) *J. Magn. Reson., Ser. B 104*, 89−94.
24. Prakash, V., and Timasheff, S. N. (1991) *Biochemistry 30*, 873−880.
25. Na, G. C., and Timasheff, S. N. (1980) *Biochemistry 19*, 1355−1365.
26. Na, G. C., and Timasheff, S. N. (1986) *Biochemistry 25*, 6214−6222.
27. Li, Y., Edsall, R., Jr., Jagtap, P. G., Kingston, D. G., and Bane, S. (2000) *Biochemistry 39*, 616−623.
28. Han, Y., Chaudhary, A. G., Chordia, M. D., Sackett, D. L., Perez-Ramirez, B., Kingston, D. G., and Bane, S. (1996) *Biochemistry 35*, 14173−14183.
29. Prakash, V., and Timasheff, S. N. (1985) *Biochemistry 24*, 5004−5010.
30. Bhattacharyya, B., and Wolff, J. (1976) *Proc. Natl. Acad. Sci. U.S.A. 73*, 2375−2378.
31. Na, G. C., and Timasheff, S. N. (1980) *Biochemistry 19*, 1347−1354.
32. Lobert, S., Boyd, C. A., and Correia, J. J. (1997) *Biophys. J. 72*, 416−427.
33. Wilson, L., Jordan, M. A., Morse, A., and Margolis, R. L. (1982) *J. Mol. Biol. 159*, 125−149.
34. Singer, W. D., Jordan, M. A., Wilson, L., and Himes, R. H. (1989) *Mol. Pharmacol. 36*, 366−370.
35. Jordan, M. A., Margolis, R. L., Himes, R. H., and Wilson, L. (1986) *J. Mol. Biol. 187*, 61−73.

BI026182M